



Status and developments of target production for research on heavy and superheavy nuclei and elements

Bettina Lommel^{1,a} , Christoph E. Düllmann^{1,2,3}, Birgit Kindler¹, Dennis Renisch^{2,3}

¹ GSI Helmholtzzentrum für Schwerionenforschung GmbH, Planckstraße 1, 64291 Darmstadt, Germany

² Department Chemie - Standort TRIGA, Johannes Gutenberg-Universität Mainz, Fritz-Strassmann-Weg 2, 55128 Mainz, Germany

³ Helmholtz-Institut Mainz, Staudingerweg 18, 55128 Mainz, Germany

Received: 2 September 2022 / Accepted: 18 December 2022 / Published online: 2 February 2023

© The Author(s) 2023

Communicated by Nicolas Alamanos

Abstract We give an overview of the special challenges regarding target development and production for accelerator-based heavy and superheavy-nuclei experiments in the past and perspectives for the future. Production of ever heavier elements, studies of heavy-element production in fusion or transfer reactions, spectroscopic investigations on their nuclear structure and decay and on the fission processes with fragment analyses, laser spectroscopic studies of their atomic structure, high-precision mass measurements as well as chemical studies are lively fields of current science. The ever-increasing beam intensities, feasible with new accelerator development, are crucial for the synthesis of superheavy elements because of the low cross sections for many of the reactions. Therefore, the development of target and backing materials with higher durability and experiment lifetime is increasingly important. Here we concentrate on the techniques necessary for the production of targets that are needed for experiments in this special field of interest. For the future, also development on target monitoring, target cooling, and beam intensity profile shaping techniques will play an important role, but are not in the focus of this article.

1 Introduction

Uranium is the last element with an almost stable isotope. The production of heavy elements (HE) beyond uranium is possible via neutron-capture in high-flux reactors [1]. This pathway reaches a natural limit at fermium (atomic number $Z=100$), as this element does not feature any β^- -decaying isotope leading to the next heavier element. In this report, we concentrate on experiments for production and investigation of elements and isotopes beyond fermium, which are

accessible in heavy-ion reactions. The interest in such elements increased in the 1960s when predictions based on the nuclear shell model suggested the existence of an “island of stability” of superheavy elements (SHE), the nuclei which owe their existence to the influence of nuclear shell effects, see e.g. [2,3]. Recent advances in the production of SHE have been reviewed, see e.g. [4–6] and citations therein.

In the past decades, several research centres played crucial roles to advance the production and study of superheavy elements. We focus here on the program at GSI Darmstadt, Germany, where SHE studies have been a pillar of the research program for decades (a recent overview highlighting element discovery and chemical studies can be found in [7]) and also a lively nuclear spectroscopy program has been continuously conducted, see e.g. [8–12]. More recently, high-precision mass measurements with the SHIPTRAP double-Penning trap system [13,14] and laser spectroscopic studies [15] were advanced to the region of transfermium isotopes at GSI, see also [16,17].

Experiments to synthesize new heavy elements with small cross sections essentially follow two different reaction paths that were dubbed “hot” and “cold” fusion reactions depending on the magnitude of the lowest achievable excitation energies (or temperature) of the compound nuclei. In both reaction paths, choosing reaction partners with closed nucleon shells proved to be most favourable for the cross section of the evaporation residues. Therefore, for cold-fusion reactions ^{208}Pb , which is the heaviest and most neutron-rich doubly-magic isotope, is the preferred target material in combination with the most neutron-rich stable isotope of the complementary element giving the wanted compound nucleus. For the synthesis of odd- Z elements, ^{209}Bi is the preferred target material. With cold-fusion reactions the elements $Z = 107$ – 112 were synthesized at GSI in Darmstadt, Germany [18] and element 113 at RIKEN, Wako, Japan [19]. In the so-

^a e-mail: b.lommel@gsi.de (corresponding author)

called hot-fusion reactions, in which the compound nucleus is formed at higher excitation energy, actinide targets are used and are irradiated (i) with light projectiles to produce the early transfermium elements, and (ii) with the doubly-magic ^{48}Ca to produce the heaviest currently known elements. With this method, elements 112–118 were synthesized at FLNR in Dubna, Russia [20–23]. For a summary of the discovery of the SHE we refer to Hofmann et al. [18] and Oganessian et al. [24] and citations therein.

We divided this report roughly into two parts according to the quite different methods for preparation and handling issues for abundant stable or quasi-stable isotopes on the one hand and the rare highly radioactive actinides on the other hand. We structure the paper along the different production techniques and preparation methods. A general overview to methods of target preparation for particle accelerators is given, e.g., in [25]. Some of the current challenges and advances for their mitigation are discussed in [26]. We will give a brief overview on the different sorts of experiments and the targets potentially required. We will end with some future perspectives.

2 Stable target materials

The technique for target production has to be chosen according to the necessary active target area and homogeneity of the target layer taking into account the price and availability of the target material. The process has then to be optimized with respect to material consumption, yield, homogeneity, and beam durability of the layer wanted for the experiment. For rare or very expensive target materials, also the possibility of recovery and the achievable yield can be an issue.

In this part, we also include targets of quasi-stable natural uranium and of the isotope ^{238}U , as they can be produced by the same production processes.

2.1 Production processes

Thermal evaporation

For stable targets applied in heavy-ion experiments, the most common production method is thermal evaporation. With thermal evaporation, a yield of about 50% for a target homogeneity of $\sim \pm 5\%$ and a target thickness up to $\sim 1\text{ mg/cm}^2$ can be reached. Thermal evaporation works well for most elements and compounds where the melting temperature is not too high.

A necessary condition for thermal evaporation is the availability of a crucible material that does not react or alloy with the target material until the evaporation temperature is reached. Typical crucible materials are molybdenum, platinum, tantalum, and tungsten, which have very high melting

temperatures and are not or only slowly reacting with most of the relevant target materials.

In thermal evaporation the target material has to be deposited either on a backing that is compatible with the experiment or on a substrate from which the target layer can be removed after deposition. In general, for the experiments relevant in the frame of this report, low- Z backings are suitable. We will refer to the backing question in Sect. 4, since this is a major issue also for actinide targets discussed in Sect. 3.

Thermal evaporation is a process that works under high vacuum to prevent any contamination of the target layer with impurities from the residual gas. The amount of target material needed for the required layer thickness is placed in the crucible that is clamped between electrodes. Especially for isotopically enriched targets, the required amount of starting material is determined before in test series with material of natural isotopic composition. The geometry of the process, especially the distance of the crucible, from which evaporation occurs isotropically into 2π geometry, and the target backing, is always a compromise between the homogeneity of the target layer and the yield of the process (consumption of material). It has to be optimized for each material taking into account the demands of the respective experiment. To increase the yield without loss in layer homogeneity the substrate is often rotated above the evaporation source during the process.

As an example, we describe in the following our standard setup for the production of targets for the Separator for Heavy-Ion reaction Products (SHIP) at GSI [27]. To dissipate the heat induced by the pulsed beam of GSI's UNILAC accelerator, the target wheel technique is employed. Here one 5-ms long beam pulse irradiates one of eight target segments mounted on the target wheel that rotates synchronously with the beam [28]. The size of the targets and the distribution and profile of the beam were improved continuously [29]. A similar technique is employed at the TransActinide Separator and Chemistry Apparatus (TASCA) [30], albeit with a different target wheel geometry [31]. For the production of targets for TASCA, the geometry in the deposition setup is adjusted accordingly. Similar setups can be found more or less modified in many target laboratories working in this field with stable isotopes, see e.g. [32–34].

For the production of standard targets for the heavy-element program, we use evaporation wheels very similar to the target wheels actually applied for the experiments at SHIP and TASCA. On each wheel, eight, respectively four banana-shaped target frames with appropriate backing foils are mounted. In Fig. 1 such an evaporation wheel for SHIP, already installed in the coating unit, is shown. In general, carbon foils with a thickness of $\sim 30\text{--}100\ \mu\text{g/cm}^2$ are applied as a backing for the targets discussed here. For special applications, backings with thicknesses of up to $10\ \mu\text{m}$ out of

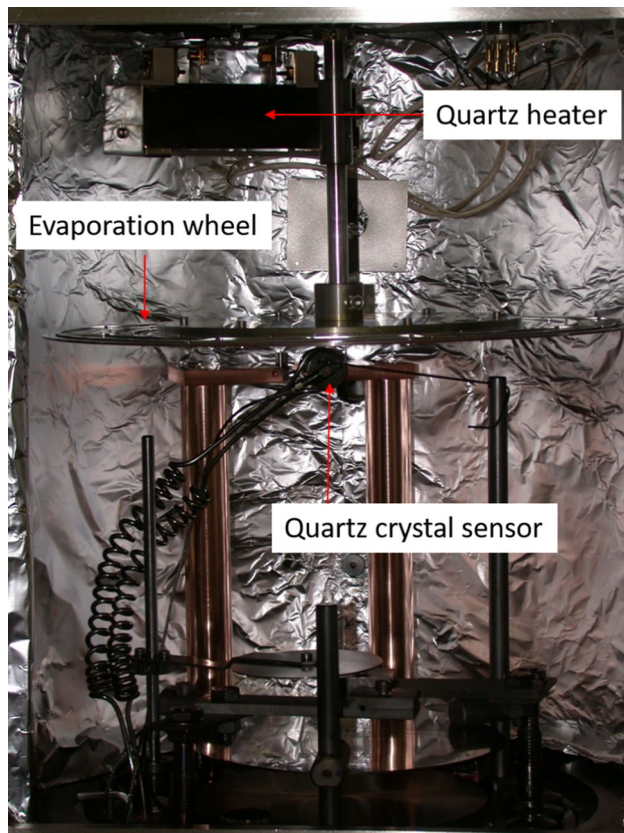


Fig. 1 Evaporation wheel for SHIP setup mounted in the vacuum coater

aluminium, beryllium or titanium can be chosen as well. For metal backings nevertheless the behaviour in deposition, the yield, the sticking behaviour and the durability in the beam can differ.

Figure 2 shows a detailed view of Fig. 1. The crucible is clamped between the copper electrodes and a part of the evaporation wheel with a carbon backing on a target frame is visible in the gap directly above the opening of the crucible. In the front, the quartz crystal sensor is mounted to monitor the evaporation process. Quartz crystal sensors operate on the principle of inverse piezoelectric effect in which an alternating voltage applied across the crystal surfaces causes it to vibrate at its natural frequency. When the quartz crystal gets coated during evaporation the frequency changes. This change in frequency is then converted to a layer thickness by suitable calibration.

The crucible, usually made of tantalum, is heated until the target material evaporates. During the process, the evaporation wheel is rotated above the opening of the crucible. Before starting the real production run with isotopic material, we test the setup and optimize the yield of the process with natural material. For this, the initial weight of target material needed to achieve the required target thickness by evaporating the material until the crucible is empty, is determined.

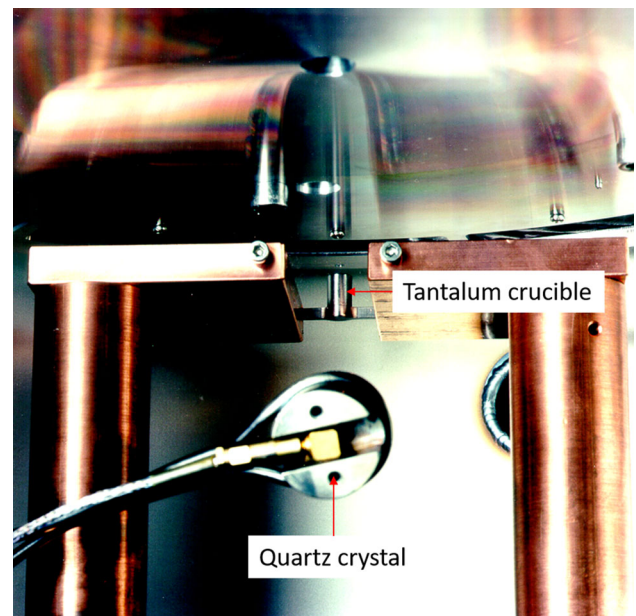


Fig. 2 Detail of Fig. 1. Tantalum crucible clamped between the copper electrodes and the evaporation wheel mounted closely above the opening of the crucible

Then we calculate the resulting thickness of each test run by weighing the target frames with the backing before and after the coating process. We use the quartz-crystal sensor only to monitor the start and the end of the evaporation process. The process ends with a rapid drop of the evaporation rate, which indicates that all target material has been evaporated. Often, the target layer is afterwards coated with a covering layer of $5\text{--}10\ \mu\text{g}/\text{cm}^2$ of carbon to reduce a sputtering of the target layer by the impinging particle beam. Depending on the obtained structure of the target material, it can be necessary to heat the backside of the backing to transform the deposited layer into a compact homogenous layer. Therefore, we can heat the backing up to $250\ ^\circ\text{C}$ with a quartz heater situated above the target wheel, as can be seen in Fig. 1.

Direct current magnetron sputtering For materials with high melting temperatures or high reactivity direct current (DC) magnetron sputtering with a low-density argon plasma can be an alternative production method since sputtering is a ballistic process that works independently of the vapour pressure of the material. The method is also an option for compounds that tend to decompose during heating.

In Fig. 3, a vacuum chamber with a sputtering setup is shown. On the left photograph, a 1-inch magnetron source with a shutter and a rotatable target wheel for the substrates is shown in the front. A 3-inch magnetron applied for other processes is situated in the back. The photograph in the right panel shows a close-up of the magnetron with a mounted sputter target that was already in use for some time.

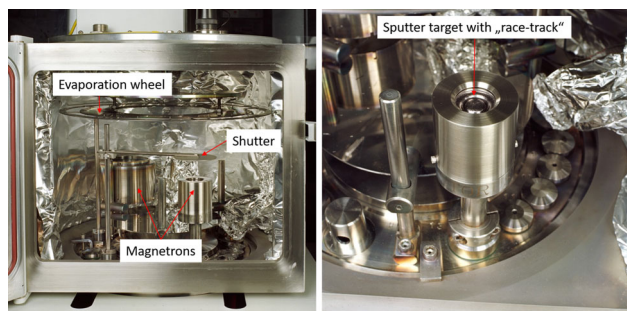


Fig. 3 Left—Vacuum chamber with the target wheel, a shutter and the 1-inch magnetron source in the front. Right—Detail view of the magnetron with a mounted sputter target

To start the process, an argon plasma is ignited between the outer shield of the magnetron, which acts as an anode, and the sputtering target acting as a cathode. A magnetic field created from permanent magnets below the sputter target together with the vertical electric field confines the low-pressure plasma to a torus above the sputter cathode, as shown schematically in Fig. 4 for a Torus™ magnetron source. The Ar-ions from the plasma zone are accelerated towards the cathode, knocking out particles from the sputter target. Because of the geometry of the magnetic field, the ablation from the sputter target mainly takes place in a ring-shaped area resulting in the “race-track” visible on the sputter target in Fig. 3 on the right.

As a rule of thumb, the minimum distance between the sputter target and the substrate should be of the same order as the diameter of the sputter source applied to avoid damage of the substrate by the plasma. This distance is also necessary to ensure a satisfactory homogeneity of the target layer. This rather large gap results in an only medium efficiency in terms of material consumption.

As in thermal evaporation, the target wheel with the mounted backings is rotated above the magnetron during the ablation process. One major difficulty in magnetron sputtering is that the target material has to be available in form of a thick foil or a sheet with the diameter of the magnetron. Moreover, from this rather large amount of material only a small amount in the “race-track” region is usable for the process.

In SHE-experiments, this method is applied successfully for metallic uranium and UO_2 [35]. Magnetron sputtering was also tested for ^{198}Pt but in the end cold rolling proved to be the more feasible and effective method for this very rare isotope, as described in detail in the following paragraph.

Cold rolling Cold rolling is a purely mechanical process that can be applied only to metals, which are rollable, i.e., the material is neither too hard nor too brittle. As starting material either a bead or a thick foil is required. If the target material is only available as a powder or in small pieces, it has

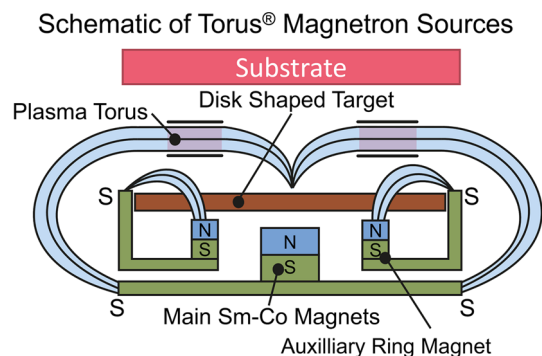


Fig. 4 Schematic principle of a planar Torus™ Magnetron (Figure by courtesy of Kurt J. Lesker company)

to be molten to a bead in advance. The thus prepared starting material is placed between scratch-free annealed stainless steel plates and this sandwich is then step-by-step rolled down until the target foil reaches the required thickness. The velocity of the rollers is adapted to the rolling process; the stainless steel plates are changed as required. The width of the rollers must be at least three times the width of the sheets to be rolled to reach a homogeneity over the target area better than $\pm 5\%$. Rolled targets can be recovered to nearly 100%, only in the re-melting process some material loss occurs.

However, with this method a target thickness of maximum $\sim 500 \mu\text{g}/\text{cm}^2$ as is mostly the wanted thickness for experiments with the heaviest elements is often not achievable pinhole-free for target areas of several cm^2 . The cold rolling process is applied mainly for the production of metallic backings, see Sect. 4. The process can also be favourable for targets made from metallic isotopes that are either very rare or not readily available on the world market.

2.2 Target materials

Lead and bismuth targets As explained in the introduction, for cold-fusion reactions ^{208}Pb and ^{209}Bi are the preferred target nuclei. This reaction class has been employed over decades at GSI, mainly for the discovery of new elements, for nuclear spectroscopic studies, and more recently also for laser spectroscopy and high-precision mass spectrometry. Therefore, a lot of development work was performed on these two materials over more than two decades to enhance the durability of the targets in the beam.

For lead and bismuth as target materials, the major challenges are the low melting temperatures of the metals of 327°C and 271°C , respectively. Therefore, in the past we synthesized and tested several compounds of lead and bismuth with higher melting temperatures [29,36,37]. Now, mostly PbS with a melting temperature of 1114°C and Bi_2O_3 with a melting temperature of 817°C are applied as target materials in case the expected beam intensities are too high

for the metals. To ensure a smooth and homogenous deposition of PbS the backing is heated up to 250 °C with a quartz lamp during the thermal evaporation process as described above.

Rare-earth targets Many rare-earth elements are interesting target materials for studies in nuclear spectroscopy of heavy elements, as well as in chemical studies, where superheavy elements are produced in the irradiation of actinide targets, and the irradiation of the homologue rare earth leads to the production of the lighter homologue of the superheavy element, see [38–41] for recent examples.

In principle, for many experiments the metals are the favourite form since additional nuclei only increase the background signals. However, enriched rare-earth materials are not always available as metal. Depending on the melting temperature, not all rare-earth metals can be deposited thermally from the crucible. Furthermore, the rare-earth metals differ in their sensitivity for oxidization in air. All these factors determine if the metal or a compound is applied as target material. At the GSI target laboratory, producing rare-earth fluoride targets is often the alternative of choice if a metallic target cannot be produced or if the metal cannot be handled.

Enriched rare-earth materials are usually available on the market as oxides, sometimes also as metals. In principle, for both deposition with an electron beam gun is possible. However, with this process only a yield between ~ 2 and 5% is achievable which is no option for enriched target material. Converting the rare-earth oxide into the metal is almost never an option as the yield of such a process also is very low. As the rare-earth oxides have a very high melting temperature they cannot be deposited thermally, but have to be chemically converted into the fluoride. All rare-earth fluorides can be deposited thermally from a tantalum crucible onto carbon backings.

The rare-earth fluorides are stable in air. Here, a carbon covering-layer is recommended as well to reduce sputtering during the experiment. The left panel of Fig. 5 shows $^{142}\text{NdF}_3$ with a thickness of about $250 \mu\text{g}/\text{cm}^2$ deposited on $\sim 45 \mu\text{g}/\text{cm}^2$ carbon on a SHIP target frame mounted on the wheel, which runs in the experiment. The right panel shows metallic natural neodymium with a thickness of about $240 \mu\text{g}/\text{cm}^2$ deposited on $2.2 \mu\text{m}$ titanium on a banana-shaped target frame fixed on the target wheel as it was employed in nuclear chemistry experiments.

Uranium targets Another material, which is applied quite often in SHE-experiments, is uranium as a cross-over to the actinides. At the GSI target laboratory, natural uranium or depleted ^{238}U , with their low radioactivity, can be handled more or less like a stable material with the only precaution that the preparation takes place in a radiation surveillance area. Uranium targets from other isotopes can be produced at

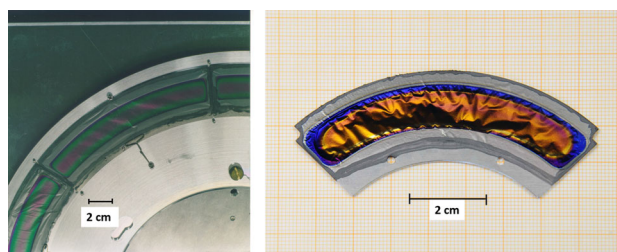


Fig. 5 Left—Target on a SHIP-wheel: $\sim 250 \mu\text{g}/\text{cm}^2$ $^{142}\text{NdF}_3$ on $\sim 45 \mu\text{g}/\text{cm}^2$ carbon backing. Right—A TASCA-target with $\sim 240 \mu\text{g}/\text{cm}^2$ metallic natural neodymium on $2.2 \mu\text{m}$ titanium backing

Johannes Gutenberg University Mainz (JGU) with the methods available there, see Sect. 3.

Here, we focus on uranium target production at GSI. In the past, uranium was mostly applied either as the metal or as the fluoride, UF_4 . With thermal evaporation, only the compound UF_4 with a melting temperature of 1036 °C was successfully produced, as described in Sect. 2.1. These targets are stable against oxidation and ageing but are not very stable during irradiation [42].

Although the melting temperature of metallic uranium with 1133 °C is not significantly higher compared to the fluoride, thermal evaporation of the metal is not feasible because of the fast oxidation. Therefore, metallic uranium targets are produced by DC magnetron sputtering, as described in Sect. 2.1. However, metallic uranium-targets have to be handled in dry air and even then, they tend to oxidize and degrade rapidly.

In principle, uranium oxide and uranium carbide, which have melting temperatures above 2000 °C and are stable in air, could both be suitable uranium compounds for SHE-targets. But UO_2 was chosen as it has a defined stoichiometry, does not decompose during the deposition process or the irradiation and can be sintered into solid bulk material. If the corresponding sputter target is available targets from metallic uranium, uranium oxide and uranium carbide can be produced by magnetron sputtering. Procuring sputter targets of uranium or uranium oxide is difficult since there are only few companies working with uranium at all and manufacturing such parts in small numbers is economically not interesting for most companies.

Platinum targets Targets of highly enriched ^{198}Pt or ^{196}Pt are also of interest for SHE-experiments since they are neutron-rich and heavy. But they are a very special case from the point of view of target production. As enriched platinum material cannot be produced with the gas-centrifuge technique but only with a calutron, there are just two production sites worldwide, one in the US and one in Russia. Which isotopes are enriched with these separators and whether the obtained isotope is sold worldwide is a research policy decision of the respective country. For this reason, e.g., ^{198}Pt has been

practically unavailable on the world market for many years. Therefore, the scarce material available on stock is applied only in the metallic form without a backing in order to guarantee the recovery of the material. Once evaporated, e.g., on carbon backing, it cannot be recovered easily without major carbon impurities.

For this reason, cold rolling as described in Sect. 2.1 is the process of choice for this material, although it is an extremely lengthy and tedious procedure. Nevertheless, targets with a thickness of down to 1.5 mg/cm^2 could be produced by cold rolling and were applied successfully in several experiments [43–45].

The rollability of a material crucially depends on the manufacturing process and the purity of the starting material. Any inclusions or impurities can make the cold rolling process extremely difficult or even impossible.

Other materials The variety of target materials that are of interest for specific experiments with heavy and superheavy nuclei is much wider; usually, the neutron-rich isotopes of heavier metals are most desirable candidates. Most of those targets can be produced by thermal evaporation as well.

Toxic materials like osmium or thallium for example are problematic to handle in standard laboratories. In principle, such targets can be produced with thermal evaporation, as described by Gehlot et al. for Tl-isotopes [46] and citations therein, but special safety measures have to be provided. They can also be produced with electrochemical methods as for example described by Frémont et al. for osmium [47]. For most of these toxic materials also for the application in the experiments the safety conditions have to be checked!

Targets from materials where the metal and the known compounds are volatile or unstable to heating or ion bombardment, like mercury for example, are also difficult to produce with thermal evaporation. Here, an extensive testing of compounds and their durability has to be performed before production of the targets from the isotope can start.

2.3 Quality control and analytics

In general, the target frame with the mounted backing foil is weighed before the coating process and afterwards with the target material. The difference of the weights together with the known size of the coated area yields the mean areal thickness of the target layer. To get an overview of the spatial distribution of target thickness, representative targets are cut to small quadratic pieces and are weighed very precisely thus mapping the whole target area.

Additionally, all targets are inspected visually for holes, cracks or other conspicuous features. Targets with defects are either discarded or, in case of only minor defects, saved as spare ones. In the case of developing and testing new compounds, the structure of the target layer is inspected by opti-

cal microscopy and with a Scanning Electron Microscope (SEM). Furthermore, with Energy Dispersive X-Ray (EDX) analysis the stoichiometry of the layer can be verified and possible impurities from the crucible material can be identified.

3 Actinide targets

The preparation of actinide targets involves additional challenges compared to the preparation of targets of (quasi)stable isotopes. Due to the short half-lives of some nuclides, high activities may need to be handled. Accordingly, manufacturing processes are needed that are safe for workers from a radiation safety perspective and prevent contamination of laboratory equipment. Another aspect of handling actinides is often the low availability of certain nuclides. In some cases, only enough material for a single set of targets is available [48]. A high reliability of the method, a high deposition yield and the possibility to recover and reprocess non-deposited material as well as irradiated targets are relevant prerequisites. All these requirements severely limit the number of methods available, with electrochemical deposition methods usually being the most suitable.

3.1 Molecular plating (MP)

An electrochemical approach called “molecular plating” (MP) [49] is an established method that fulfils requirements mentioned in the former paragraph. The method is based on an electrochemical deposition of material dissolved in alcoholic solution by applying a constant current density (typically in the range of about 0.8 mA/cm^2) between an anode and the supporting substrate, which is biased as cathode, as shown in Fig. 6 left. By adapting parameters like the applied current and the deposition time, the method is capable of producing homogeneous layers of various actinide elements from uranium up to californium, see Fig. 6 right, with thicknesses up to about 1 mg/cm^2 and yields of 90% or even more in a single deposition step [50–53].

Thin foils of beryllium, carbon, tantalum, or platinum have been used as substrates in the past. On the one hand the backing should be as thin as possible to reduce unwanted side-reactions and to minimize the energy-loss of the ion beam and hence the beam-induced heating that might eventually destroy the target. On the other hand the backing has to provide sufficient mechanical stability and thermal resistance to guarantee the survival of the target layer during the deposition process, the handling as well as during the irradiation process. Titanium foils of about $2.2 \text{ }\mu\text{m}$ thickness were established in the last decade, because they offer a good compromise of those requirements. See also Sect. 4 as well as [26] for more

detailed considerations about advantages and disadvantages of different backing materials.

3.2 Analytics

The first characterization step of an actinide target is the determination of the deposition yield and the layer thickness. Important analytical techniques to determine the yield of the deposition are α - or γ -spectroscopic measurements. Depending on the type of radionuclide, this is done either of the finished target (direct determination) or of the radionuclide content remaining in the supernatant solution after the plating (indirect determination). In cases where inactive material is deposited, e.g. lanthanides for test purposes, or where the resulting activity is too low for a meaningful measurement due to a long half-life of the applied radionuclide, neutron activation analysis (NAA) can be used to create short-living γ -emitters in the supernatant solution, which can be used for yield determination. It should be noted that the MP process leads to the co-deposition of other species in addition to the isotope of interest, which also contribute to the actual layer thickness [54]. For a full characterization, these in general unwanted co-deposited species as well as the chemical form of the deposited material have to be identified [55].

A qualitative analysis of the homogeneity of the target can be performed by radiographic imaging (RI) [56] Fig. 7, resulting in grey-scale pictures of the activity distribution on the substrate. Those pictures can be post-processed to obtain false-colour pictures or even 3D plots with the height representing the local activity for a clear visualization of the activity distribution.

Microscopic techniques, like Atomic Force Microscopy (AFM) or SEM, as shown in Fig. 8, can provide additional structural information about the target layer. However, those

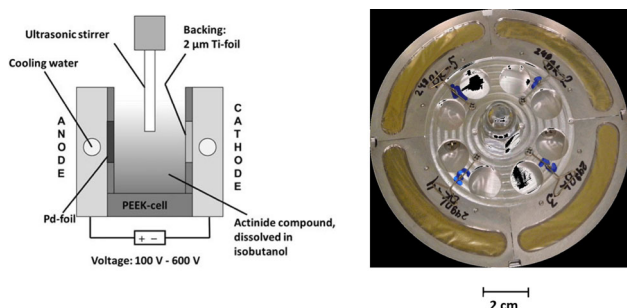


Fig. 6 Left: Schematic drawing of a typical setup for actinide deposition by molecular plating. Right: Assembled TASCA target wheel with 4 target segments, containing a total amount of about 12 mg ^{249}Bk , deposited by molecular plating on 2- μm thick Ti-backings [52] (Reprinted by permission from Springer Nature Customer Service Centre GmbH: Springer Berlin Heidelberg, Journal of Radioanalytical and Nuclear Chemistry, Preparation of actinide targets for the synthesis of the heaviest elements, J. Runke et al., J. Radioanal. Nucl. Chem. 299 (2014) 1081, Copyright ©2013, Akadémiai Kiadó, Budapest, Hungary)

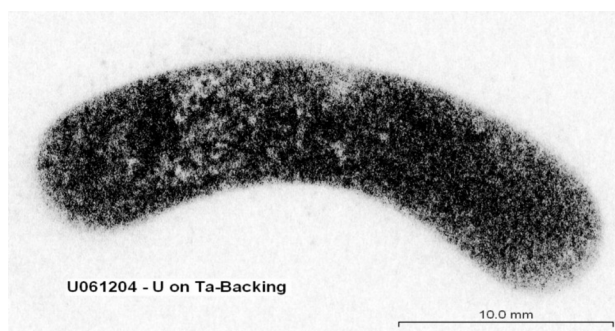


Fig. 7 Radiographic imaging of an uranium target with a thickness of $410 \mu\text{g}/\text{cm}^2$ on a tantalum backing [57]

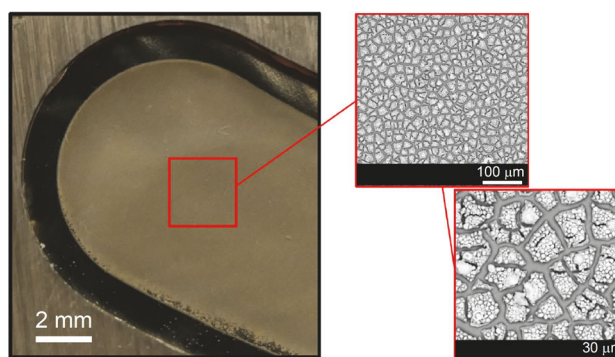


Fig. 8 Photograph (left) and SEM pictures (centre and right) of a $500 \mu\text{g}/\text{cm}^2$ ^{147}Sm target on a TASCA segment

methods do only reveal information about a small area of the whole target layer, which might be a drawback if no sufficiently representative sections of the target are selected. AFM can be used to reveal the morphology and roughness either of the pure substrate or of the finished target on a (sub)micrometre scale [54]. Especially the impact of different pre-treatments of the substrate, like cleaning and etching procedures, can be monitored this way and correlated with differences in the resulting deposit layer. A SEM allows taking detailed pictures of representative structures on the target, as depicted in Fig. 8, helping to benchmark the influence of certain plating parameters, like the used solvent, current density, or H_2O and CO_2 content in the plating solution. Beside the sole optical information, a SEM can also be applied for further analytics, like elemental analysis by using an EDX detector. This way, the characteristic X-rays of the elements present in the sample can be measured, leading to a qualitative and quantitative elemental analysis of the constituents [56,58]. Further information is accessible via Raman spectroscopy, as first studies with lead films show [59–61].

To characterize the chemical environment and composition of a target layer, methods such as X-ray photoelectron spectroscopy (XPS), Infrared (IR) or Raman spectroscopy are available. XPS investigations have shown that significant amounts of different carbon species are part of the layer in classical MP deposits. As the source of these species, the

deposition of solvent fragments or electrochemical side reactions caused by the applied high voltages have been considered [62,63]. Direct thickness measurements on nanometre scale using 3D laser microscopic methods are promising to have a direct access to this central value, but have not been established as a standard analysis tool for actinide targets up to now.

3.3 Recent advances

Although molecular plating has been used for many decades in the superheavy element community, many of the underlying mechanisms involved in thin-layer production as well as the exact nature of beam-induced modifications are not fully understood yet. In the past decade, the interest in elucidating these questions have become of field of more interest, e.g. [54,63–67].

At JGU, recent investigations of lead and various lanthanide targets by IR and confocal Raman spectroscopy have revealed the presence of carbonate and formate species in the target layers. The composition of the layer changes significantly upon intense irradiation with an ion beam. For example, a lead layer consisting of the carbonate $(\text{PbCO}_3)_2$ after production is converted to α -PbO during the irradiation with a 5.90 MeV/u ^{48}Ca -beam [68]. Those analytics aim for a better understanding of the plating process itself and the development of new target production methods, superior to classical molecular plating, like the adoption of more modern electrochemical approaches, already known in literature for lanthanide chemistry [69–71]. Such methods have the potential to give access to thicknesses of more than 1 mg/cm^2 , to avoid unwanted structural inhomogeneity, caused e.g. by mud-cracking effects during the drying process [72], and to provide for layers with a better defined chemical structure.

One such approach could be the coordination of the solved actinide ions as tosylate [73] or triflate [74–76] complexes prior to the deposition. This would open the possibility to work in water-free solvents like DMF, being the basic requirement for a deposition of the metallic form of the target material [68]. Another approach could be the introduction of conducting salts, which are nowadays often applied in state-of-the-art electrochemical processes. They provide the advantage to operate with significantly lower potentials at the working electrode, leading to a suppression of unwanted side reactions, so that a chemically better defined layer could be gained [77].

4 Backings

Targets that cannot be manufactured self-supporting require a thin film as backing. For an appropriate choice of the backing, the following requirements need to be considered [26]:

- Material with a low Z is preferable, to minimize the production of α -emitting isotopes in the interaction between projectile and the backing material that would contribute to unwanted background. These experiments often rely on the unambiguous identification of single nuclei of the heaviest elements via detection of their radioactive decay, mostly α -decay.
- To minimize the straggling and the energy loss in the backing the backing layer should be as thin as possible without losing too much in mechanical stability.
- Mechanical and thermal stability is needed for an acceptable handling and good durability in the beam. This is especially important for rare and/or highly-radioactive actinides.
- To guarantee a good adhesion of the target material to the backing, the thermal expansion coefficient of the backing material should be as similar as possible to that of the deposited target material.
- There must not be any chemical reaction between target material and backing material.

In general, these criteria are fulfilled best for beryllium, carbon, aluminium, and titanium. For the heavy-element experiments at TASCA first systematic studies for backings compatible with MP were performed in 2008 [78]. For targets produced with thermal evaporation carbon is mostly the material of choice. Among the mentioned materials, carbon has the lowest thermal expansion and can be produced rather thin compared to all alternatives.

Thin carbon layers can be produced by sputtering, by arc heating, by resistance heating and by laser ablation. The thinnest carbon foils with the highest homogeneity are prepared by resistance heating. Standard backing for bismuth and lead targets is amorphous carbon. The carbon is produced by resistive heating of ultrapure graphite electrodes on glass plates coated with betaine sucrose as a water-soluble interlayer [79].

For actinide targets that are primarily produced by MP, the mechanical stability of the backing material plays a major role. Therefore in this case, carbon is no reliable option up to now, and beryllium, titanium or aluminium are the preferred materials.

Beryllium backings have to be purchased in the required thickness, as the safety precautions for cold rolling or machining beryllium are very high and only a few companies worldwide are producing beryllium.

Metallic aluminium and titanium backings are mostly produced by cold rolling, as described previously in Sect. 2.1. Pinhole-free aluminium and titanium can be produced in a thickness range from ~ 2 to $10 \mu\text{m}$ with thickness homogeneity better than $\pm 2\%$. The obtained foils are cut and glued with carbon glue based on butyl acetate or with a two-component

conductive epoxy glue, depending on the subsequent production process for the target.

5 Target monitoring

The durability of the targets during irradiation is crucial. Loss in target material results in a reduction of the production rate and especially in case of radioactive targets, lost material is sometimes impossible to replace and will in addition lead to contamination of the target chamber. Even if sufficient material is available for the production of spare targets, target exchange always costs valuable beam time. This motivates the monitoring of the integrity and thickness of the targets online or at least a verification of the target thickness offline either while interrupting the irradiation or subsequent to the experiment.

A direct online monitoring of the integrity and the thickness of the targets is most favourable. Many experiments detect the beam particles that are elastically scattered in forward direction for this purpose, as described already by Ref. [80].

Mann et al. [81] developed an online target monitoring system to measure thickness and structural properties of the targets with a much higher spatial resolution. It is based on the attenuation of an electron beam penetrating the target layer opposite to the beam position. With this method, each target can be scanned for pin-hole formation or degradation online. The spatial resolution is in the order of 0.5 mm. This method was successfully applied in experiments at SHIP, see e.g. [82] and was also integrated in the LISE-spectrometer at GANIL [83, 84]. The method is protected by an international patent under PCT [85].

At the GAs-filled Recoil Ion Separator (GARIS) at RIKEN the energy spectrum of beam particles elastically scattered from the target is monitored by a PIN photodiode at a scattering angle of 45° and is used to monitor the intensity of the beam and the condition of the target foils [33]. A similar technique is used at the Berkeley Gas-filled Separator (BGS) at Lawrence Berkeley National Laboratory, Berkeley, CA, USA [86].

Another method for monitoring the target thickness is measuring the attenuation of α -particles passing the target layer. For target material with a significant α -activity, the decrease of activity is a direct measure for the loss of target material. For other materials, the attenuation of α -particles of an α -source passing the target layer can be used. Still, here the irradiation has to be interrupted for the monitoring procedure.

In addition, a monitoring of the target temperature is mandatory. This can be done with spot measurements with a pyrometer or an IR sensor or by thermal imaging of the whole target with an ultra-fast IR camera.

At TASCA the target wheel control system, the beam control at the experimental site and the monitoring of the target behaviour were consolidated in a single control system in a feedback loop as these measurements are interacting with each other [31].

6 Outlook

Continuing to improve the durability of the targets so that they can withstand more intense heavy ion beams for a reasonable period remains a major challenge. For individual conventional materials or their compounds, it may be useful to transfer the electrolytic deposition processes up to now only applied for the production of actinide targets because of the much higher yield. It will also be important for the future to identify suitable higher-melting compounds for individual materials.

Reducing isotopic rare-earth oxides in small quantities with high yields will be of importance for nuclear spectroscopy. For all parameters mentioned above like durability, homogeneity, stability and yield there is still large room for improvement and simulation of variation in experimental parameters on the target temperature is essential [87]. Close monitoring during the experiment is becoming increasingly important for higher beam intensities. Especially for separators running under vacuum like SHIP, a direct cooling can be an option, as already shown by studies in mock-up experiments [36, 88].

Acknowledgements The authors thank the staff of the target laboratories of GSI, Elif Celik Ayik, Annett Hübner, Jutta Steiner and Vera Yakusheva and of JGU Mainz, Klaus Eberhardt, Christoph Mokry, Jörg Runke, Petra Thörle-Pospiech, and Norbert Trautmann for their dedicated work in the past and the present. Many thanks to Michael Block, Fritz-Peter Heßberger, Sebastian Raeder for their scientific counseling and help with appropriate references, and Ernst Artes and Carl-Christian Meyer for fruitful discussions. We thank Gabi Otto for most of the photographs. The publication is funded by the Deutsche Forschungsgemeinschaft (DFG, German Research Foundation) - 491382106, and by the Open Access Publishing Fund of GSI Helmholtzzentrum fuer Schwerionenforschung.

Funding Information Open Access funding enabled and organized by Projekt DEAL.

Data availability This manuscript has associated data in a data repository. [Authors' comment: This manuscript has associated data in data repositories as indicated in the references.]

Open Access This article is licensed under a Creative Commons Attribution 4.0 International License, which permits use, sharing, adaptation, distribution and reproduction in any medium or format, as long as you give appropriate credit to the original author(s) and the source, provide a link to the Creative Commons licence, and indicate if changes were made. The images or other third party material in this article are included in the article's Creative Commons licence, unless indicated otherwise in a credit line to the material. If material is not included in the article's Creative Commons licence and your intended

use is not permitted by statutory regulation or exceeds the permitted use, you will need to obtain permission directly from the copyright holder. To view a copy of this licence, visit <http://creativecommons.org/licenses/by/4.0/>.

References

- J.B. Roberto, C.W. Alexander, R.A. Boll, J.D. Burns, J.G. Ezold, L.K. Felker, S.L. Hogle, K.P. Rykaczewski, Actinide targets for the synthesis of super-heavy elements. *Nucl. Phys. A* **944**, 99 (2015). <https://doi.org/10.1016/j.nuclphysa.2015.06.009>
- W.D. Myers, W.J. Swiatecki, Nuclear masses and deformations. *Nucl. Phys.* **81**, 1 (1966). [https://doi.org/10.1016/S0029-5582\(66\)80001-9](https://doi.org/10.1016/S0029-5582(66)80001-9)
- A. Sobiczewski, F.A. Gareev, B.N. Kalinkin, Closed shells for $Z > 82$ and $N > 126$ in a diffuse potential well. *Phys. Lett.* **22**, 500 (1966). [https://doi.org/10.1016/S0029-5582\(66\)80001-9](https://doi.org/10.1016/S0029-5582(66)80001-9)
- S. Hofmann, Synthesis of superheavy elements by cold fusion. *Radiochim. Acta* **99**, 405 (2011). <https://doi.org/10.1524/ract.2011.1854>
- Y.T. Oganessian, V.K. Utyonkov, Superheavy nuclei from ^{48}Ca -induced reactions. *Nucl. Phys. A* **944**, 62 (2015). <https://doi.org/10.1016/j.nuclphysa.2015.07.003>
- Eds: Ch.E. Düllmann, R.-D. Herzberg, W. Nazarewicz, Yu. Oganessian, Special issue on superheavy elements. *Nucl. Phys. A* **944** (2015)
- Ch.E. Düllmann, M. Block, F.P. Heßberger, J. Khuyagbaatar, B. Kindler, J.V. Kratz, B. Lommel, G. Münzenberg, V. Pershina, D. Renisch, M. Schädel, A. Yakushev, Five decades of GSI superheavy element discoveries and chemical investigation. *Radiochim. Acta* **110**(6–9), 417 (2022). <https://doi.org/10.1515/ract-2022-0015>
- F.P. Heßberger, Nuclear structure investigations in the region of Superheavy Nuclei. *Phys. At. Nucl.* **70**, 1445 (2007). <https://doi.org/10.1134/S1063778807080200>
- J. Khuyagbaatar, H.M. Albers, M. Block, H. Brand, R.A. Cantemir, A. Di Nitto, Ch.E. Düllmann, M. Götz, S. Götz, F.P. Heßberger, E. Jäger, B. Kindler, J.V. Kratz, J. Krier, N. Kurz, B. Lommel, L. Lens, A. Mistry, B. Schausten, J. Uusitalo, A. Yakushev, Search for electron-capture delayed fission in the new isotope ^{244}Md . *Phys. Rev. Lett.* **125**, 142504 (2020). <https://doi.org/10.1103/PhysRevLett.125.142504>
- J. Khuyagbaatar, H. Brand, R.A. Cantemir, Ch.E. Düllmann, F.P. Heßberger, E. Jäger, B. Kindler, J. Krier, N. Kurz, B. Lommel, B. Schausten, A. Yakushev, Spontaneous fission instability of the neutron-deficient No and Rf isotopes: the new isotope ^{249}No . *Phys. Rev. C* **104**, L031303 (2021). <https://doi.org/10.1103/PhysRevC.104.L031303>
- A. Sårmark-Roth, D.M. Cox, D. Rudolph, L.G. Sarmiento, B.G. Carlsson, J.L. Egidio, P. Golubev, J. Heery, A. Yakushev, S. Åberg, H.M. Albers, M. Albertsson, M. Block, H. Brand, T. Calverley, R. Cantemir, R.M. Clark, Ch.E. Düllmann, J. Eberth, C. Fahlander, U. Forsberg, J.M. Gates, F. Giacoppo, M. Götz, S. Götz, R.-D. Herzberg, Y. Hrabar, E. Jäger, D. Judson, J. Khuyagbaatar, B. Kindler, I. Kojouharov, J.V. Kratz, J. Krier, N. Kurz, L. Lens, J. Ljungberg, B. Lommel, J. Louko, C.-C. Meyer, A. Mistry, C. Mokry, P. Papadakis, E. Parr, J.L. Pore, I. Ragnarsson, J. Runke, M. Schädel, H. Schaffner, B. Schausten, D.A. Shaughnessy, P. Thörle-Pospiech, N. Trautmann, J. Uusitalo, Spectroscopy along flerovium decay chains: discovery of ^{280}Ds and an excited State in ^{282}Cn . *Phys. Rev. Lett.* **126**, 032503 (2021). <https://doi.org/10.1103/PhysRevLett.126.032503>
- M. Block, F. Giacoppo, F.-P. Heßberger, S. Raeder, Recent progress in experiments on the heaviest nuclides at SHIP. *Riv. Nuovo Cim.* **45**, 279 (2022). <https://doi.org/10.1007/s40766-022-00030-5>
- M. Block, D. Ackermann, K. Blaum, A. Chaudhuri, Z. Di, S. Eliseev, R. Ferrer, D. Habs, F. Herfurth, F.P. Heßberger, S. Hofmann, H.-J. Kluge, G. Maero, A. Martín, G. Marx, M. Mazzocco, M. Mukherjee, J.B. Neumayr, W.R. Plaß, W. Quint, S. Rahaman, C. Rauth, D. Rodríguez, C. Scheidenberger, L. Schweikhard, P.G. Thirolf, G. Vorobjev, C. Weber, Towards direct mass measurements of nobelium at SHIPTRAP. *Eur. Phys. J. D* **45**, 39 (2007). <https://doi.org/10.1140/epjd/e2007-00189-2>
- O. Kaleja, B. Andelić, K. Blaum, M. Block, P. Chetri, C. Droese, Ch.E. Düllmann, M. Eibach, S. Eliseev, J. Even, S. Götz, F. Giacoppo, N. Kalantar-Nayestanaki, M. Laatiaoui, E. Minaya Ramirez, A. Mistry, T. Murböck, S. Raeder, L. Schweikhard, P.G. Thirolf, *Nucl. Inst. Meth. B* **463**, 280 (2020). <https://doi.org/10.1016/j.nimb.2019.05.009>
- M. Block, M. Laatiaoui, S. Raeder, Recent progress in laser spectroscopy of the actinides. *Prog. Part. Nucl. Phys.* **116**, 103834 (2021). <https://doi.org/10.1016/j.pnpnp.2020.103834>
- M. Block, Precise ground state properties of the heaviest elements for studies of their atomic and nuclear structure. *Radiochim. Acta* **107**, 603 (2019). <https://doi.org/10.1515/ract-2019-0002>
- M. Block, Direct mass measurements and ionization potential measurements of the actinides. *Radiochim. Acta* **107**, 821 (2019). <https://doi.org/10.1515/ract-2019-3143>
- S. Hofmann, G. Münzenberg, The discovery of the heaviest elements. *Rev. Modern Phys.* **72**, 733 (2000). <https://doi.org/10.1103/RevModPhys.72.733>
- K. Morita, K. Morimoto, D. Kaji, T. Akiyama, S. Goto, H. Haba, E. Ideguchi, R. Kanungo, K. Katori, H. Koura, H. Kudo, T. Ohnishi, A. Ozawa, T. Suda, K. Sueki, H. Xu, T. Yamaguchi, A. Yoneda, A. Yoshida, Y. Zhao, Experiment on the synthesis of element 113 in the reaction $^{209}\text{Bi}(^{70}\text{Zn}, n)^{278}113$. *J. Phys. Soc. Jpn.* **73**, 2593 (2004). <https://doi.org/10.1143/JPSJ.73.2593>
- Yu. Oganessian, A.V. Yeremin, A.G. Popeko, S.L. Bogomolov, G.V. Buklanov, M.L. Chelnokov, V.I. Chepigin, B.N. Gikal, V.A. Gorshkov, G.G. Gulbekian, M.G. Itkis, A.P. Kabachenko, A.Y. Lavrentev, O.N. Malyshev, J. Rohac, R.N. Sagaidak, S. Hofmann, S. Saro, G. Giardina, K. Morita, Synthesis of nuclei of the superheavy element 114 in reactions induced by ^{48}Ca . *Nature* **400**, 242 (1999). <https://doi.org/10.1038/22281>
- Yu. Ts, V.K. Oganessian, S.N. Utyonkov, Y.V. Dmitriev, M.G. Lobanov, A.N. Itkis, Y.S. Plyakov, A.N. Tsyganov, A.V. Mezentsev, A.A. Yeremin, E.A. Voinov, G.G. Sokol, S.L. Gulbekian, S. Bogomolov, V.G. Iliev, A.M. Subbotin, G.V. Sukhov, S.V. Buklanov, V.I. Shishkin, G.K. Chepygin, N.V. Vosokin, M. Aksenov, K. Hussonnois, V.I.Z. Subotic, Synthesis of elements 115 and 113 in the reaction $^{243}\text{Am} + ^{48}\text{Ca}$. *Phys. Rev. C* **72**, 034611 (2005). <https://doi.org/10.1103/PhysRevC.72.034611>
- Yu. Ts, V.K. Oganessian, Y.V. Utyonkov, F.S. Lobanov, A.N. Abdullin, R.N. Polyakov, I.V. Sagaidak, Y.S. Shirokovsky, A.A. Tsyganov, G.G. Voinov, S.L. Gulbekian, B.N. Bogomolov, A.N. Gikal, S. Mezentsev, V.G. Iliev, A.M. Subbotin, K. Sukhov, V.I. Subotic, G.K. Zagrebaev, M.G.I. Vostokin, Synthesis of the isotopes of elements 118 and 116 in the ^{249}Cf and $^{245}\text{Cm} + ^{48}\text{Ca}$ fusion reactions. *Phys. Rev. C* **74**, 044602 (2006). <https://doi.org/10.1103/PhysRevC.74.044602>
- Yu. Ts, F.S. Oganessian, P.D. Abdullin, D.E. Bailey, M.E. Benker, S.N. Bennett, J.G. Dmitriev, J.H. Ezold, R.A. Hamilton, M.G. Henderson, Y.V. Itkis, A.N. Lobanov, K.J. Mezentsev, S.L. Moody, A.N. Nelson, C.E. Polyakov, A.V. Porter, F.D. Ramayya, J.B. Riley, M.A. Roberto, K.P. Ryabinkin, R.N. Rykaczewski, D.A. Sagaidak, I.V. Shaughnessy, M.A. Shirokovsky, V.G. Stoyer, R. Subbotin, A.M. Sudowe, Y.S. Sukhov, V.K. Tsyganov, A.A. Utyonkov, G.K. Voinov, P.A.W. Vostokin, Synthesis of a new element with atomic number $Z = \frac{1}{4} 117$. *Phys. Rev. Lett.* **104**, 142502 (2010). <https://doi.org/10.1103/PhysRevLett.104.142502>

24. Yu. Ts, O.V.K. Utyonkov, Super-heavy element research. Rep. Prog. Phys. **78**, 036301 (2015). <https://doi.org/10.1088/0034-4885/78/3/036301>
25. B. Lommel, B. Kindler, Targets for particle accelerators, digital encyclopedia of applied physics. Wiley Online Library (2009). <https://doi.org/10.1002/3527600434.eap494.pub2>
26. Ch.E. Düllmann, E. Artes, A. Dragoun, R. Haas, E. Jäger, B. Kindler, B. Lommel, K.-M. Mangold, C.-C. Meyer, C. Mokry, F. Munnik, M. Rapps, D. Renisch, J. Runke, A. Seibert, M. Stöckl, P. Thörle-Pospiech, C. Trautmann, N. Trautmann, A. Yakushev, Advancements in the fabrication and characterization of actinide targets for superheavy element production. J. Radioanal. Nucl. Chem. (2022). <https://doi.org/10.1007/s10967-022-08631-4>
27. G. Münzenberg, W. Faust, S. Hofmann, P. Armbruster, K. Güttner, H. Ewald, The velocity filter ship, a separator of unslowed heavy ion fusion products. Nucl. Instr. Method **161**, 65 (1979). [https://doi.org/10.1016/0029-554X\(79\)90362-8](https://doi.org/10.1016/0029-554X(79)90362-8)
28. S. Hofmann, New elements - approaching $Z = 114$. Rep. Prog. Phys. **61**, 639 (1998). <https://doi.org/10.1088/0034-4885/61/6/002>
29. B. Lommel, D. Gembalies-Datz, W. Hartmann, S. Hofmann, B. Kindler, J. Klemm, J. Kojouharova, J. Steiner, Improvement of the target durability for heavy-element production. Nucl. Instr. Method. Phys. Res. A **480**, 16 (2002). [https://doi.org/10.1016/S0168-9002\(01\)02041-1](https://doi.org/10.1016/S0168-9002(01)02041-1)
30. A. Semchenkov, W. Bröchle, E. Jäger, E. Schimpf, M. Schädel, C. Mühle, F. Klos, A. Türler, A. Yakushev, A. Belov, T. Belyakova, M. Kaparkova, V. Kukhtin, E. Lamzin, S. Sytchevsky, The Trans-Actinide Separator and Chemistry Apparatus (TASCA) at GSI — optimization of ion-optical structures and magnet designs. Nucl. Instr. Method Phys. Res. B **266**, 4153 (2008). <https://doi.org/10.1016/j.nimb.2008.05.132>
31. E. Jäger, H. Brand, Ch.E. Düllmann, J. Khuyagbaatar, J. Krier, M. Schädel, T. Torres, A. Yakushev, High intensity target wheel at TASCA: target wheel control system and target monitoring. J. Radioanal. Nucl. Chem. **299**, 1073 (2014). <https://doi.org/10.1007/s10967-013-2645-1>
32. J.P. Greene, A. Heinz, J. Falout, R.V.F. Janssens, Rotating target wheel system for super-heavy element production at ATLAS. Nucl. Instr. Method. Phys. Res. A **521**, 214 (2004). <https://doi.org/10.1016/j.nima.2003.11.411>
33. A. Yoshida, K. Morita, K. Morimoto, D. Kaji, T. Kubo, Y. Takahashi, A. Ozawa, I. Tanihata, High-power rotating wheel targets at RIKEN. Nucl. Instr. Method. Phys. Res. A **521**, 65 (2004). <https://doi.org/10.1016/j.nima.2003.11.408>
34. Ch. Stodel, G. Frémont, G. Auger, C. Spitaels, First steps towards a target laboratory at GANIL. Nucl. Instr. Method Phys. Res. A **561**, 112 (2006). <https://doi.org/10.1016/j.nima.2005.12.233>
35. B. Lommel, E. Celik Ayik, A. Hübner, B. Kindler, J. Steiner, V. Yakusheva, Uranium targets for heavy-ion accelerators, EPJ Web of Conferences **229**, 03006 (2020), <https://doi.org/10.1051/epjconf/202022903006>
36. B. Kindler, S. Antalic, H.-G. Burkhard, P. Cagarda, D. Gembalies-Datz, W. Hartmann, S. Hofmann, J. Kojouharova, J. Klemm, B. Lommel, R. Mann, S. Saro, H.-J. Schött, J. Steiner, Status of the target development for the heavy element program. AIP Conf. Proc. **576**, 1148 (2001). <https://doi.org/10.1063/1.1395508>
37. B. Kindler, D. Ackermann, W. Hartmann, F.P. Heßberger, S. Hofmann, B. Lommel, R. Mann, J. Steiner, Chemical compound targets for SHIP on heated carbon backings. Nucl. Instr. Method. Phys. Res. A **561**, 107 (2006). <https://doi.org/10.1016/j.nima.2005.12.232>
38. A. Yakushev, J.M. Gates, A. Türler, M. Schädel, Ch.E. Düllmann, D. Ackermann, L.-L. Andersson, M. Block, W. Bröchle, J. Dvorak, K. Eberhardt, H.G. Essel, J. Even, U. Forsberg, A. Gorshkov, R. Graeger, K.E. Gregorich, W. Hartmann, R.-D. Herzberg, F.P. Heßberger, D. Hild, A. Hübner, E. Jäger, J. Khuyagbaatar, B. Kindler, J.V. Kratz, J. Krier, N. Kurz, B. Lommel, L.J. Niewisch, H. Nitsche, J.P. Omtvedt, E. Parr, Z. Qin, D. Rudolph, J. Runke, B. Schausten, E. Schimpf, A. Semchenkov, J. Steiner, P. Thörle-Pospiech, J. Uusitalo, M. Wegrzecki, N. Wiehl, Superheavy element flerovium (Element 114) is a volatile metal. Inorg. Chem. **53**, 1624 (2014). <https://doi.org/10.1021/ic4026766>
39. L. Lens, A. Yakushev, Ch.E. Düllmann, M. Asai, J. Ballof, M. Block, H.M. David, J. Despotopoulos, A. Di Nitto, K. Eberhardt, J. Even, M. Götz, S. Götz, H. Haba, L. Harkness-Brennan, F.P. Heßberger, R.D. Herzberg, J. Hoffmann, A. Hübner, E. Jäger, D. Judson, J. Khuyagbaatar, B. Kindler, Y. Komori, J. Konki, J.V. Kratz, J. Krier, N. Kurz, M. Laatiaoui, S. Lahiri, B. Lommel, M. Maiti, A.K. Mistry, C. Mokry, K. Moody, Y. Nagame, J.P. Omtvedt, P. Papadakis, V. Pershina, J. Runke, M. Schädel, P. Scharrer, T. Sato, D. Shaughnessy, B. Schausten, P. Thörle-Pospiech, N. Trautmann, K. Tsukada, J. Uusitalo, A. Ward, M. Wegrzecki, N. Wiehl, V. Yakusheva, Online chemical adsorption studies of Hg, Tl, and Pb on SiO₂ and Au surfaces in preparation for chemical investigations on Cn, Nh, and Fl at TASCA. Radiochim. Acta **106**, 949 (2018). <https://doi.org/10.1515/ract-2017-2914>
40. A. Yakushev, L. Lens, Ch.E. Düllmann, M. Block, H. Brand, T. Calverley, M. Dasgupta, A. Di Nitto, M. Götz, S. Götz, H. Haba, L. Harkness-Brennan, R.-D. Herzberg, F.P. Heßberger, D. Hinde, A. Hübner, E. Jäger, D. Judson, J. Khuyagbaatar, B. Kindler, Y. Komori, J. Konki, J.V. Kratz, J. Krier, N. Kurz, M. Laatiaoui, B. Lommel, C. Lorenz, M. Maiti, A.K. Mistry, Ch. Mokry, Y. Nagame, P. Papadakis, A. Sámarm-Roth, D. Rudolph, J. Runke, L.G. Sarmiento, T.K. Sato, M. Schädel, P. Scharrer, B. Schausten, J. Steiner, P. Thörle-Pospiech, A. Toyoshima, N. Trautmann, J. Uusitalo, A. Ward, M. Wegrzecki, V. Yakusheva, First study on Nihonium (Nh, Element 113) chemistry at TASCA. Front. Chem. **9**, 1 (2021). <https://doi.org/10.3389/fchem.2021.753738>
41. A. Yakushev, L. Lens, Ch.E. Düllmann, J. Khuyagbaatar, E. Jäger, J. Krier, J. Runke, H.M. Albers, M. Asai, M. Block, J. Despotopoulos, A. Di Nitto, K. Eberhardt, U. Forsberg, P. Golubev, M. Götz, S. Götz, H. Haba, L. Harkness-Brennan, R.-D. Herzberg, F.P. Heßberger, D. Hinde, A. Hübner, D. Judson, B. Kindler, Y. Komori, J. Konki, J.V. Kratz, N. Kurz, M. Laatiaoui, S. Lahiri, B. Lommel, M. Maiti, A.K. Mistry, Ch. Mokry, K.J. Moody, Y. Nagame, J.P. Omtvedt, P. Papadakis, V. Pershina, D. Rudolph, L.G. Sarmiento, T.K. Sato, M. Schädel, P. Scharrer, B. Schausten, D.A. Shaughnessy, J. Steiner, P. Thörle-Pospiech, A. Toyoshima, N. Trautmann, K. Tsukada, J. Uusitalo, K.-O. Voss, A. Ward, M. Wegrzecki, N. Wiehl, E. Williams, V. Yakusheva, On the adsorption and reactivity of element 114, flerovium. Front. Chem. **10**, 976635 (2022). <https://doi.org/10.3389/fchem.2022.976635>
42. B. Kindler, D. Ackermann, W. Hartmann, F.-P. Heßberger, S. Hofmann, A. Hübner, B. Lommel, R. Mann, J. Steiner, Uranium fluoride and metallic uranium as target materials for heavy-element experiments at SHIP. Nucl. Instr. Methods A **590**, 126 (2008). <https://doi.org/10.1016/j.nima.2008.02.031>
43. P. Cagarda, S. Antalic, S. Saro, S. Hofmann, F.P. Heßberger, D. Ackermann, B. Kindler, B. Lommel, J. Kojouharova, R. Mann, H.H. Schött, The new isotopes ²³³Cm and ²³⁴Cm, Proceedings of the 5th International Conference on Dynamical Aspects of Nuclear Fission, 23–27. (October 2001), World Scientific Publishing Co. Pte. Ltd
44. P. Cagarda, Synthesis and properties of neutron deficient transuranium nuclei, Ph.D. thesis, Comenius University Bratislava (2002)
45. F.P. Heßberger, GSI experiments on synthesis and nuclear structure investigations of the heaviest nuclei. Eur. Phys. J. D **45**, 33 (2007). <https://doi.org/10.1140/epjd/e2007-00146-1>
46. J. Gehlot, S.R. Abhilash, S. Ojha, D. Mehta, D. Kabiraj, A.M. Vinodkumar, Fabrication and characterization of carbon-backed ^{203,205}Tl targets. J. Radioanal. Nucl. Chem. **305**, 755 (2015). <https://doi.org/10.1007/s10967-015-4100-y>

47. G. Frémont, Y. Ngono-Ravache, C. Schmitt, Ch. Stodel, Preparation of osmium targets with carbon backing. *AIP Conf. Proc.* **1962**, 030002 (2018). <https://doi.org/10.1063/1.5035519>
48. J. Khuyagbaatar, A. Yakushev, Ch.E. Düllmann, D. Ackermann, L.-L. Andersson, M. Asai, M. Block, R.A. Boll, H. Brand, D.M. Cox, M. Dasgupta, X. Derkx, A. Di Nitto, K. Eberhardt, J. Even, M. Evers, C. Fahlander, U. Forsberg, J.M. Gates, N. Gharibyan, P. Golubev, K.E. Gregorich, J.H. Hamilton, W. Hartmann, R.-D. Herzberg, F.P. Heßberger, D.J. Hinde, J. Hoffmann, R. Hollinger, A. Hübner, E. Jäger, B. Kindler, J.V. Kratz, J. Krier, N. Kurz, M. Laatiaoui, S. Lahiri, R. Lang, B. Lommel, M. Maiti, K. Miernik, S. Minami, A.K. Mistry, C. Mokry, H. Nitsche, J.P. Omtvedt, G.K. Pang, P. Papadakis, D. Renisch, J.B. Roberto, D. Rudolph, J. Runke, K.P. Rykaczewski, L.G. Sarmiento, M. Schädel, B. Schausten, A. Semchenkov, D.A. Shaughnessy, P. Steinegger, J. Steiner, E.E. Tereshatov, P. Thörle-Pospiech, K. Tinschert, T. Torres De Heidenreich, N. Trautmann, A. Türlér, J. Uusitalo, M. Wegrzecki, N. Wiehl, S.M. Van Cleve, V. Yakusheva, Search for elements 119 and 120. *Phys. Rev. C* **102**, 064602 (2020). <https://doi.org/10.1103/PhysRevC.102.064602>
49. W. Parker, R. Falk, Molecular plating: a method for the electrolytic formation of thin inorganic films. *Nucl. Instr. Methods* **16**, 355 (1962). [https://doi.org/10.1016/0029-554X\(62\)90142-8](https://doi.org/10.1016/0029-554X(62)90142-8)
50. N. Trautmann, H. Folger, Preparation of actinide targets by electrodeposition. *Nucl. Instr. Methods A* **282**, 102 (1989). [https://doi.org/10.1016/0168-9002\(89\)90117-4](https://doi.org/10.1016/0168-9002(89)90117-4)
51. K. Eberhardt, W. Brüchle, Ch.E. Düllmann, K.E. Gregorich, W. Hartmann, A. Hübner, E. Jäger, B. Kindler, J.V. Kratz, D. Liebe, B. Lommel, H.-J. Maier, M. Schädel, B. Schausten, E. Schimpf, A. Semchenkov, J. Steiner, J. Szerypo, P. Thörle, A. Türlér, A. Yakushev, Preparation of targets for the gas-filled recoil separator TASCAs by electrochemical deposition and design of the TASCAs target wheel assembly. *Nucl. Instr. Methods Phys. Res. A* **590**, 134 (2008). <https://doi.org/10.1016/j.nima.2008.02.069>
52. J. Runke, Ch.E. Düllmann, K. Eberhardt, P.A. Ellison, K.E. Gregorich, S. Hofmann, E. Jäger, B. Kindler, J.V. Kratz, J. Krier, B. Lommel, C. Mokry, H. Nitsche, J.B. Roberto, K.P. Rykaczewski, M. Schädel, P. Thörle-Pospiech, N. Trautmann, A. Yakushev, Preparation of actinide targets for the synthesis of the heaviest elements. *J. Radioanal. Nucl. Chem.* **299**, 1081 (2014). <https://doi.org/10.1007/s10967-013-2616-6>
53. K. Eberhardt, Ch.E. Düllmann, R. Haas, C. Mokry, J. Runke, P. Thörle-Pospiech, N. Trautmann, Actinide targets for fundamental research in nuclear physics. *AIP Conf. Proceed.* **1962**, 030009 (2018). <https://doi.org/10.1063/1.5035526>
54. A. Vascon, S. Santi, A.A. Isse, T. Reich, J. Drebert, H. Christ, Ch.E. Düllmann, K. Eberhardt, Elucidation of constant current density molecular plating. *Nucl. Instr. Methods Phys. Res. A* **696**, 180 (2012). <https://doi.org/10.1016/j.nima.2012.08.072>
55. C. Stodel, Methods of targets' characterization. *EPJ Web Conf.* **229**, 02001 (2020). <https://doi.org/10.1051/epjconf/202022902001>
56. D. Liebe, K. Eberhardt, W. Hartmann, T. Häger, A. Hübner, J.V. Kratz, B. Kindler, B. Lommel, P. Thörle, M. Schädel, J. Steiner, The application of neutron activation analysis, scanning electron microscope, and radiographic imaging for the characterization of electrochemically deposited layers of lanthanide and actinide elements. *Nucl. Instr. Methods Phys. Res. A* **590**, 145 (2008). <https://doi.org/10.1016/j.nima.2008.02.075>
57. D. Liebe, K. Eberhardt, J.V. Kratz, W. Hartmann, A. Huebner, B. Kindler, B. Lommel, J. Steiner, *Improvements at the radiographic analysis of radioactive targets* (Ann. Rep. Nuclear Chemistry Mainz, 2006)
58. S. Sadi, A. Paulenova, P.R. Watson, W. Loveland, Growth and surface morphology of uranium films during molecular plating. *Nucl. Instr. Methods Phys. Res.* **655**, 80 (2011). <https://doi.org/10.1016/j.nima.2011.06.025>
59. R. Haas, C.-C. Meyer, S. Böhland, Ch.E. Düllmann, J. Mäder, K. Tinschert, ODIIn - A setup for Off-line Deposit Irradiations of thin layers for nuclear physics applications. *Nucl. Instr. Methods Phys. Res. A* **957**, 163366 (2020). <https://doi.org/10.1016/j.nima.2019.163366>
60. C.-C. Meyer, A. Dragoun, C.E. Düllmann, R. Haas, E. Jäger, B. Kindler, B. Lommel, A. Prosvetov, M. Rapps, D. Renisch, P. Simon, M. Tomut, C. Trautmann, A. Yakushev, Chemical conversions in lead thin films induced by heavy-ion beams at Coulomb barrier energies. *Nucl. Instr. Methods Phys. Res. A* **1028**, 166365 (2022). <https://doi.org/10.1016/j.nima.2022.166365>
61. C.L. Tracy, M. Lang, F. Zhang, Ch. Trautmann, R.-C. Ewing, Phase transformations in Ln₂O₃ materials irradiated with swift heavy ions. *Phys. Rev. B* **92**, 174101 (2015). <https://doi.org/10.1103/PhysRevB.92.174101>
62. A. Vascon, N. Wiehl, T. Reich, J. Drebert, K. Eberhardt, C.E. Düllmann, The performance of thin layers produced by molecular plating as alpha-particle sources. *Nucl. Instr. Methods Phys. Res. A* **721**, 35 (2013). <https://doi.org/10.1016/j.nima.2013.04.050>
63. K. Myhre, J. Delashmitt, N. Sims, S. Van Cleve, R. Boll, Samarium thin films molecular plated from N, N-dimethylformamide characterized by XPS. *Surf. Sci. Spectra* **25**, 024003 (2018). <https://doi.org/10.1116/1.5052011>
64. S.N. Dmitriev, A.G. Popeko, High-power radioactive targets as one of the key problems in further development of the research program on synthesis of new superheavy elements. *J. Radioanal. Nucl. Chem.* **305**, 927 (2015). <https://doi.org/10.1007/s10967-014-3920-5>
65. W. Loveland, L. Yao, D.M. Asner, R.G. Baker, J. Bundgaard, E. Burgett, M. Cunningham, J. Deaven, D.L. Duke, U. Greife, S. Grimes, M. Heffner, T. Hill, D. Isenhower, J.L. Klay, V. Kleinrath, N. Kornilov, A.B. Laptev, T.N. Massey, R. Mehrarchand, H. Qu, J. Ruz, S. Sangiorgio, B. Selhan, L. Snyder, S. Stave, G. Tishvili, R.T. Thornton, F. Tovesson, D. Towell, R.S. Towell, S. Watson, B. Wendt, L. Wood, Targets for Precision Measurements. *Nuclear Data Sheets* **119**, 383 (2014). <https://doi.org/10.1016/j.nds.2014.08.106>
66. W. Loveland, High quality actinide targets. *J. Radioanal. Nucl. Chem.* **307**, 1591 (2016). <https://doi.org/10.1007/s10967-015-4337-5>
67. J. Choi, Y. H. Chung, Preparation of Lanthanum Oxide and Lanthanum Oxy carbonate Layers on Titanium by Electrodeposition with Organic Solution. *J. of Nanomat.* **2016** ID 5140219 (2016). <https://doi.org/10.1155/2016/5140219>
68. C.-C. Meyer, E. Artes, M. Bender, J. Brötz, Ch.E. Düllmann, C. Haese, E. Jäger, B. Kindler, B. Lommel, M. Major, M. Rapps, D. Renisch, F. Munnik, C. Trautmann, A. Yakushev, Production and irradiation of Lanthanide targets with high surface weights. *Nucl. Instr. Meth. Phys. Res. A*, to be published (2022)
69. D. Melo, G. Vicentini, L. Zinner, Synthesis, Properties and Structure of Hexaquo-tris(N, N-dimethylformamide)-lanthanide Trifluoromethanesulfonates. *Inorganica Chimica Acta* **146**, 123 (1988). [https://doi.org/10.1016/S0020-1693\(00\)80038-9](https://doi.org/10.1016/S0020-1693(00)80038-9)
70. M. Yang, D. Crerar, D. Irish, A Raman spectroscopic study of lead and zinc acetate complexes in hydrothermal solutions. *Geochimica et Cosmochimica Acta* **53**, 319 (1989). [https://doi.org/10.1016/0016-7037\(89\)90384-0](https://doi.org/10.1016/0016-7037(89)90384-0)
71. P. Schumacher, J. Doyle, J. Schenk, S. Clark, Electroanalytical chemistry of lanthanides and actinides. *Rev. Anal. Chem.* **32**, 159 (2013). <https://doi.org/10.1515/revac-2012-0032>
72. A. Vascon, S. Santi, A.A. Isse, A. Kühnle, T. Reich, J. Drebert, K. Eberhardt, Ch.E. Düllmann, Smooth crack-free targets for nuclear applications produced by molecular plating. *Nucl. Instr. Methods*

- Phys. Res. A **714**, 163 (2013). <https://doi.org/10.1016/j.nima.2013.03.003>
73. P. Liu, Q. Yang, Y. Tong, Y. Yang, Electrodeposition of Gd-Co film in organic bath. *Electrochimica Acta* **45**, 2147 (2000). [https://doi.org/10.1016/S0013-4686\(99\)00434-X](https://doi.org/10.1016/S0013-4686(99)00434-X)
 74. M.E.M. Hamidi, J.-L. Pascal, Synthesis and structural characterization of some anhydrous Ln(OTf)₃ complexes. *Polyhedron* **13**, 1787 (1994). [https://doi.org/10.1016/S0277-5387\(00\)80111-4](https://doi.org/10.1016/S0277-5387(00)80111-4)
 75. K. Egashira, Y. Yoshimura, H. Kanno, Y. Suzuki, TG-DTA study on the lanthanoid trifluoromethanesulfonate complexes. *J. Therm. Anal. Calorimetry* **71**, 501 (2003). [https://doi.org/10.1016/S0277-5387\(00\)80111-4](https://doi.org/10.1016/S0277-5387(00)80111-4)
 76. C. Apostolidis, B. Schimmelpfennig, N. Magnani, P. Lindqvist-Reis, O. Walter, R. Sykora, A. Morgenstern, E. Colineau, R. Caciuffo, R. Klenze, R.G. Haire, J. Rebizant, F. Bruchertseifer, T. Fanghänel, [An(H₂O)₉](CF₃SO₃)₃ (An=U-Cm, Cf): exploring their stability, structural chemistry, and magnetic behavior by experiment and theory. *Angew. Chem. Int. Ed.* **49**, 6343 (2010). <https://doi.org/10.1002/anie.201001077>
 77. J. Loder Meyer, M. Multerer, M. Zistler, S. Jordan, H.J. Gores, W. Kipferl, E. Diaconu, M. Sperl, G. Bayreuther, Electrochemical investigations, and study of magnetic properties. *J. Electrochem. Soc.* **153**, C242 (2006). <https://doi.org/10.1149/1.2172548>
 78. B. Lommel, W. Bröchle, K. Eberhardt, W. Hartmann, A. Hübner, B. Kindler, J.V. Kratz, D. Liebe, M. Schädel, J. Steiner, Backings and targets for chemical and nuclear studies of transactinides with TASCA. *Nucl. Instr. Methods A* **590**, 141 (2008). <https://doi.org/10.1016/j.nima.2008.02.045>
 79. B. Lommel, W. Hartmann, B. Kindler, J. Klemm, J. Steiner, Preparation of self-supporting carbon thin films. *Nucl. Instr. Methods Phys. Res. A* **480**, 199 (2002). [https://doi.org/10.1016/S0168-9002\(01\)02100-3](https://doi.org/10.1016/S0168-9002(01)02100-3)
 80. H. Folger, W. Hartmann, F.P. Heßberger, S. Hofmann, J. Klemm, G. Münzenberg, V. Ninov, W. Thalheimer, P. Armbruster, Developments of ¹⁷⁰Er, ^{204,206,207,208}Pb and ²⁰⁹Bi target wheels for reaction studies and synthesis of heaviest elements. *Nucl. Instr. Methods Phys. Res. A* **362**, 64 (1995). [https://doi.org/10.1016/0168-9002\(95\)00527-7](https://doi.org/10.1016/0168-9002(95)00527-7)
 81. R. Mann, D. Ackermann, S. Antalic, H.-G. Burkhard, P. Cagarda I, D. Gembalies-Datz, W. Hartmann, F.P. Heßberger, S. Hofmann, B. Kindler, P. Kuusiniemi, B. Lommel, S. Saro, H.G. Schött, J. Steiner, On-line Target Control, GSI Scientific Report 2003, GSI Report 2004-1, 224 (2004)
 82. S. Hofmann, S. Heinz, R. Mann, J. Maurer, J. Khuyagbaatar, D. Ackermann, S. Antalic, W. Barth, M. Block, H.G. Burkhard, V.F. Comas, L. Dahl, K. Eberhardt, J. Gostic, R.A. Henderson, J.A. Heredia, F.P. Heßberger, J.M. Kenneally, B. Kindler, I. Kojouharov, J.V. Kratz, R. Lang, M. Leino, B. Lommel, K.J. Moody, G. Münzenberg, S.L. Nelson, K. Nishio, A.G. Popeko, J. Runke, S. Saro, D.A. Shaughnessy, M.A. Stoyer, P. Thörle-Pospiech, K. Tinschert, N. Trautmann, J. Uusitalo, P.A. Wilk, A.V. Yeremin, The reaction ⁴⁸Ca + ²⁴⁸Cm → ²⁹⁶116* studied at the GSI-SHIP. *Eur. Phys. J. A* **48**, 62 (2012). <https://doi.org/10.1140/epja/i2012-12062-1>
 83. R. Anne, D. Bazin, A.C. Mueller, J.C. Jacmart, M. Langevin, The achromatic spectrometer LISE at GANIL. *Nucl. Instr. Methods Phys. Res. A* **257**, 215 (1987). [https://doi.org/10.1016/0168-583X\(87\)90763-4](https://doi.org/10.1016/0168-583X(87)90763-4)
 84. S. Grévy, and FULIS collaboration: N. Alamanos, N. Amara, J.C. Angeli, R. Anne, G. Auger, F. Becker, R. Dayras, A. Drouart, J.M. Fontbonne, A. Gillibert, D. Guereau, F. Hanappe, R. Hue, A.S. Lalleman, T. Legou, R. Lichtenthaler, E. Lienard, W. Mittig, F. De Oliveira, N. Orra, G. Politi, Z. Sosin, M.G. Saint-Laurent, J.C. Steckmeyer, C. Stodel, J. Tillier, R. de Tourreil, A.C.C. Villari, J.P. Wieleczko, A. Wieloch, Production of super heavy elements at GANIL: present status and perspectives, *J. Nucl. Radiochem. Sci.* **3**, 9 (2002). <https://doi.org/10.14494/jnrs2000.3.9>
 85. Inventor Rido Mann, Device and method for locally measuring the layer thickness of a sample and/or for locally modifying the thickness thereof with an electron beam, PCT No. WO 2004/031687 A1
 86. K.E. Gregorich, W. Loveland, D. Peterson, P.M. Zielinski, S.L. Nelson, Y.H. Chung, Ch.E. Düllmann, C.M. Folden III., K. Aleklett, R. Eichler, D.C. Hoffman, J.P. Omtvedt, G.K. Pang, J.M. Schwantes, S. Soverna, P. Sprunger, R. Sudowe, R.E. Wilson, H. Nitsche, Attempt to confirm superheavy element production in the ⁴⁸Ca + ²³⁸U reaction. *Phys. Rev. C* **72**, 014605 (2005)
 87. R.N. Sagaidak, Effects of beam wobbling and target rotation on the target temperature in experiments with intense heavy ion beams. *Phys. Rev. Acc. Beams* **24**, 083001 (2021). <https://doi.org/10.1103/PhysRevAccelBeams.24.083001>
 88. S. Antalic, P. Cagarda, D. Ackermann, H.-G. Burkhard, F.-P. Heßberger, S. Hofmann, B. Kindler, J. Kojouharova, B. Lommel, R. Mann, S. Saro, H.-J. Schott, Target cooling for high-current experiments at SHIP. *Nucl. Instr. Methods Phys. Res. A* **530**, 185 (2004). <https://doi.org/10.1016/j.nima.2004.04.217>